

The IL-22–oncostatin M axis promotes intestinal inflammation and tumorigenesis

In the format provided by the
authors and unedited

SUPPLEMENTARY MATERIAL AND METHODS SECTION

SUPPLEMENTARY MATERIAL AND METHODS

Histological staining of pSTAT1 and pSTAT3. Paraffin sections underwent deparaffinization, heat-induced epitope retrieval, and quenching of endogenous peroxidase with hydrogen peroxide. Sections were stained sequentially with anti-pSTAT1 (clone D4A7, CST) and anti-pSTAT3 (clone EP2147Y, Abcam), using the EnVision+ HRP polymer (Agilent) and OPAL system (Akoya Biosciences) for visualization. OPAL-520 and OPAL-570 dyes were used for pSTAT1 and pSTAT3, respectively. Nuclei were counterstained with DAPI (Sigma) and mounted with Fluoromount G (Southern Biotech). Multispectral imaging was performed with the Vectra® 3 system, and image analysis (spectral unmixing, tissue/cell segmentation, phenotyping) was done using inForm (v2.4.8). Cell frequencies were analyzed in R (v4.0.2) with phenoptr and phenoptrReports (v0.2.8).

In situ hybridization. Mouse *Osmr*, *Il22*, *Pdgfra*, and human *OSMR* mRNA were detected using the RNAscope 2.5 HD Reagent Kit-RED/BROWN (Bio-Techne). Fresh 5 µm paraffin sections were dried (60 °C, 1 h), deparaffinized, and pretreated with Target Retrieval buffer and protease. Sections were hybridized with probes for *Osmr*, *Ppib* (positive control), and *dapb* (negative control); FFPE 3T3 cells served as an additional positive control. Signal amplification and detection were performed with FastRed, nuclei were counterstained with hematoxylin, and slides were dehydrated and mounted with Histokitt using xylene. Imaging was done on an AxioImager Z1 microscope (Zeiss), with blinded evaluation. Images were contrast-adjusted in Adobe Photoshop for clarity. Signal quantification was performed using Ilastik (v1.3.2; classification, segmentation) and ImageJ (v1.48; analysis).

RNA extraction, cDNA synthesis, and qPCR. RNA from intestinal epithelial cells was extracted using QIAzol (Qiagen), with tissue either stabilized in RNA Later or directly lysed. Homogenization and phase separation were induced with chloroform, followed by isopropanol/GlycoBlue™ precipitation. RNA pellets were washed in 75% ethanol, resuspended

in RNase-free water, quantified (NanoDrop), and stored at -20°C or -80°C . For colon tissue, RNA was isolated using the Qiagen Mini RNA kit after storage in RNA Later at -80°C . cDNA was synthesized from 500 ng–1 μg RNA using the High-Capacity cDNA Reverse Transcription Kit (Applied Biosystems). qPCR was performed on diluted cDNA (1:50) using PowerUp™ SYBR™ Green or TaqMan Master Mix with UNG, and TaqMan Gene Expression Assays on a QuantStudio 5 (Applied Biosystems). Primers are listed in **Supplementary table 7**. Expression levels were normalized using the comparative CT method ($2^{-\Delta\text{CT}}$), with $\Delta\text{CT} = \text{CT (gene of interest)} - \text{CT (arithmetic mean of *Actb*)}$.

Reverse transcription of low RNA quantity. Colon-derived organoids were treated with specified cytokines, washed with PBS, and lysed in QIAzol (Qiagen) for RNA extraction. cDNA synthesis and pre-amplification were performed using the SMART-PCR method as previously described^{1,2}. Briefly, 100 ng total RNA was mixed with 1 mM dNTPs (ThermoFisher) and 10 μM oligo-dT primer (Biomers), denatured, and cooled on ice. First-strand synthesis was carried out using Maxima H minus reverse transcriptase (Invitrogen), RNasin (Promega), SuperScript VI RT (ThermoFisher), 1 M betaine (Sigma), 10 mM MgCl_2 , 1 μM ISPCR-TSO (Biomers; rGrG+G), and nuclease-free water. After RT inactivation, adapter-based PCR pre-amplification was performed using KAPA HiFi HotStart ReadyMix (KAPA), 200 nM ISPCR primers (Biomers), and nuclease-free water. The resulting cDNA was treated with Exonuclease I (NEB) per the manufacturer's instructions.

High-throughput gene expression analysis. Target-specific pre-amplification of cDNA was conducted in accordance with the protocol outlined in the Fluidigm Biomark HD manual. Sample and primer preparation were performed following the manufacturer's guidelines. Samples and primers were deposited onto a Dynamic 48x48 Array IFC-Chip and subsequently loaded into the central reaction chambers of the IFC-Chip using an IFC controller. Real-time quantitative PCR (RT-qPCR) gene expression analysis was executed using the Biomark HD system.

Single cell (sc) RNA library preparation and sequencing. The lamina propria mononuclear cells (LPMC), stromal, and epithelial cells were sorted by FACS and were individually hash-tagged per mouse group and cell type. Then, the single cell suspensions were obtained and applied to the 10x Genomics workflow for cell capturing and scRNA gene expression (GEX) and CITE-Seq library preparation using the Chromium Single Cell 5' Library & Gel Bead Kit version 2 (dual index) and the Single Cell 5' Feature Barcode Library Kit (10x Genomics). After cDNA amplification, the CITE-Seq libraries were prepared separately using the Dual Index Kit TN Set A while, the final GEX libraries were obtained after fragmentation, adapter ligation, and final Index PCR using the Dual Index Kit TT Set A. Qubit HS DNA assay kit (Life Technologies) was used for library quantification and fragment average sizes were determined using the Fragment Analyzer with the HS NGS Fragment Kit (1-6000bp) (Agilent). Furthermore, the libraries were sequenced on a NextSeq2000 device (Illumina) using the NextSeq 1000/2000 P3 reagent kits (100 Cycles, Illumina) and following the sequencing conditions recommended by 10x Genomics: read1: 26nt, read2: 90nt, index1: 10nt, index2: 10nt. The single-cell sequencing data from *H.h.* + anti-IL-10R colitis discussed in this section are deposited in NCBI's Gene Expression Omnibus and can be accessed through GEO Series accession number GSE269507.

Bulk RNA sequencing. For bulk RNA sequencing analysis of colonic tissue of IEC^{ΔOsmr}, Stroma^{ΔOsmr}, Endo^{ΔOsmr} and the respective controls, tissue was collected initially in RNA Later (Qiagen). RNA was isolated using the Qiagen Mini RNA kit (Qiagen) following the manufacturer's protocol. For the sequencing of *Villin^{creERT2} Osmr^{fl/fl}* and *Villin^{creERT2} Osmr^{fl/wt}* epithelial cells, EpCAM⁺ epithelial cells were FACS-sorted and lysed in the RLT lysis buffer and RNA was extracted using the RNeasy Micro Kit (Qiagen) according to the manufacturer's protocol. RNA integrity was assessed as per the manufacturer's guidelines. The following procedures were performed at Novogene, where sequencing was carried out on an Illumina NovaSeq 6000 sequencer to generate 150 bp paired-end reads. The bulk RNA-seq data generated

from colonic tissue and epithelial cells, as detailed in this section, have been deposited in NCBI's Gene Expression Omnibus. These data can be accessed via GEO Series accession number GSE269505 and GSE269506.

Single cell data processing. After sequencing, fastq files were processed using Cell Ranger 5.0.0 and the genome reference (refdata-gex-mm10-2020-A) annotation. The obtained count matrix was taken as an input for the data analysis with use of Seurat v4.0.1 and v5.0.1³. Hashtag sequences used to label individual mice were imported and combined. For the normalization of the data LogNormalize function was used. Seurat's default method was used for scaling. Hashtag demultiplexing (representing the three biological replicates per genotype) was performed based on Seurat's HTODemux with the parameter 'positive-quantile' at 0.99. Doublets, untagged and low quality (low UMI counts, high % of mitochondrial genes) cells were filtered out. After ranking by residual variance, 2000 variable genes were determined. 30 principal components were computed and stored. Integration of the single cell data was done using the Seurat pipeline. Next, the Harmony package v1.2.0 (<https://github.com/immunogenomics/harmony>)⁴ was also applied to integrate gene-cell matrix of epithelial in order to increase the quality of the integration. UMAP and t-distributed stochastic neighbor embedding were run using the first 20 principal components. Transcriptionally similar clusters were identified using shared nearest neighbor modularity optimization, with a resolution of 0.3. Signature genes were identified using the FindAllMarkers function in default parameter settings (only.pos = TRUE, min.pct = 0.25, logfc.threshold = 0.25). Epithelial and immune contaminants from stromal dataset were excluded from downstream analysis. The cluster with unclear gene expression profile and poor quality from LPMC dataset was also excluded from downstream analysis. Heatmaps and dotplots for the single-cell data were plotted with Seurat's DoHeatmap and DotPlot function, respectively, using default settings. Differential gene expression analysis was performed with the use of FindMarkers function (min.pct = 0.25, logfc.threshold = 0.25).

Cluster annotation. Epithelial cells were clustered into Enterocytes_1_0 (*Nr3c2*, *Vegfa*, *Duox2*), Enterocytes_1_1 (*Slc26a3*, *Slc20a1*), Enterocytes_2 (*Aqp8*, *Car4*), Enterocytes_3 (*Tm6gd1*, *Ubd*), Enterocytes_4 (*Aqp4*, *Gsdmc4*), Goblet (*Spink4*, *Agr2*, *Muc2*), Proliferating epithelial cells (*Mki67*, *Ccna2*, *Birc5*, *Cenpf*), transit-amplifying (TA) (*Hspdl*, *Lgr5*, *Hmgb2*), Enteroendocrine (*Chgb*, *Chga*, *Tph1*), Tuft (*Lrmp*, *Pou2f3*, *Sh2d6*). Stromal cells were clustered into Endothelial cells 1 (*Pecam1*, *Plvap*), Endothelial cells 2 (*Ackr1*, *Selp*), Lymphatic endothelial cells (*Lyve1*, *Ccl21a*, *Reln*), Stromal cells 1.1 (*Adamdec1*, *Sfrp1*, *Fbln1*), Stromal cells 1.2 (*Ecm1*, *Sfrp4*, *Clec3b*), Stromal cells 2 (*Bmp5*, *Col4a5*, *Sox6*), Mesothelial cells (*Upk3b*, *Msln*), Smooth muscle cells (*Acta2*, *Notch3*, *Rgs5*), Proliferating cells (*Mki67*, *Top2a*, *Prc1*), Oligodendrocytes (*Ank3*, *Plp1*, *Chl1*). Stromal cell signatures were obtained from the Kinchen et al. paper⁵. Immune cells were further sub-clustered into CD8 T cells (*Cd8a*, *Cd8b*), CD8 effector cells (*Gzmk*), CD4 T cells (*Cd4*), Tregs (*Foxp3*, *Ctla4*), $\gamma\delta$ -T cells (*Tcrp*), ILC1 (*Ncr1*, *Klre1*, *Tbx21*), ILC2 (*Gata3*, *Klrg1*, *Icos*), ILC3 (*Il22*, *Rorc*, *Il23r*), NK cells (*Eomes*, *Tbx21*, *Prfl*, *Nkg7*), Plasma cells (*Jchain*, *Derl3*, *Eaf2*), B cells (*Cd79*, *Vpreb3*, *Ms4a1*), Inflammatory Monocytes (*Thbs1*, *Cfb*, *Msr1*), Neutrophils (*Sl00a9*, *Sl00a8*, *Cxcr2*, *G0s2*), DC (*Clec9a*, *Clec10a*, *Xcr1*).

Publicly available scRNAseq datasets. Publicly available single-cell RNA sequencing datasets from Smillie et al.⁶ and Kong et al.⁷ were downloaded from <https://singlecell.broadinstitute.org/> (SCP259 and SCP1884) and analyzed using the methodology outlined in the respective publications. The expression of Osm-Osmr was analyzed using the Dotplot function from the Seurat package.

RNA isolation from tissue samples (IBDome cohort) and bulk RNA-seq analysis. RNA was isolated from biopsies taken during routine endoscopy or from resected tissues at the First Department of Medicine, Friedrich-Alexander Universität Erlangen-Nürnberg (Germany), and at the Department of Gastroenterology, Infectious Diseases and Rheumatology at the Charité – Universitätsmedizin Berlin (Germany) by using a single-use biopsy forceps (Olympus). Samples

were incubated in RNA protect reagent (RNAprotect Tissue Reagent, Qiagen) and stored at -80°C. One biopsy was thawed on ice and homogenized in RLT buffer (Qiagen) employing the TissueLyser LT (Qiagen) for RNA isolation. RNA was isolated using the RNeasy kit (Qiagen) and RNA Clean & Concentrator kit (Zymo Research). The concentration was measured at NanoDrop One/One (Thermo Fisher Scientific) and the quality (RNA integrity number, RIN) at Tape Station (Agilent). The RNA was used for bulk RNA sequencing at the NGS Competence Center Tübingen (NCCT). Paired sequencing reads were processed with the nf-core/rnaseq pipeline version 3.4⁸. In brief, reads were aligned to the GRCh38 reference genome with GENCODE v33 annotation using STAR⁹. Transcripts per million (TPM) were quantified using Salmon¹⁰ and transformed to $\log_{10}(\text{TPM}+1)$ for visualization in R.

Association Between OSMR and IL-22 Activity in IBD mucosal samples. To investigate the relationship between OSMR and IL-22 activity in IBD, we computed the correlation between gene expression and gene set enrichment scores across patients with active inflammation. The IL-22 gene set was curated from the top 50 upregulated genes in IL-22-treated organoids versus untreated conditions¹¹. For this analysis, we integrated multiple IBD cohorts: (1) the UNIFI trial cohort (GSE206285), comprising 530 ulcerative colitis (UC) patients; (2) the RISC cohort (GSE57945), including 189 Crohn's disease (CD) patients; and (3) the IBDome database, selecting inflamed patients which included 81 ileal CD, and 64 colonic UC patients; ; and (4) the Mount Sinai Crohn's and Colitis Registry (MSCCR) (GSE193677), consisting of 162 ileal CD, and 293 colonic UC samples. For the UNIFI cohort (GSE206285), RMA-normalized microarray expression data were used. The RISC cohort (GSE57945) and MSCCR cohort (GSE193677) contained raw read counts, which were further processed using the variance stabilizing transformation (VST) with DESeq2 v1.42.0. RNA-seq data from the IBDome cohort were \log_2 -transformed (TPM) and standardized to within-sample z-scores. Sample-based enrichment

analysis using the IL-22 gene set was performed for each sample with ssGSEA¹². Pearson correlation was applied to assess gene expression relationships.

Pearson correlation was applied to assess gene expression relationships.

Pathway analysis. Pathway activity was calculated across epithelial subsets with PROGENy v.1.24.0 with default parameters¹³. PROGENy is a computational method that leverages a large compendium of publicly available perturbation experiments to identify a core set of Pathway Responsive Genes (PRGs), enabling the inference of pathway activity from transcriptomic data. Pathway activities were visualized as cluster averages using the R package ComplexHeatmap¹⁴.

Prediction of cell–cell interaction with CellPhoneDB. Ligand–receptor interaction analysis was performed using the Python package CellPhoneDB (v.2.1.7, Python v.3.8.18) following instructions from the GitHub repository¹⁵. The annotated Seurat object from single cell RNA-Seq mouse data was used to test the expression of known ligand–receptor interactions from the public repository of CellPhoneDB. The dataset was downsampled to 10000 cells. Gene symbols were first converted from mouse to human using the biomaRt R package (v.2.58.2). Mean values representing the average ligand and receptor expression of annotated clusters were calculated based on the percentage of cells expressing the gene, and the gene-expression mean. To determine the significance of observed means, P values were calculated using a null distribution of means calculated for randomly permuted annotated cluster labels. An interaction was considered significant if $P \leq 0.05$. Significant interactions between enterocytes and immune cells with highest expression of Osm were extracted, gene symbols were converted from human to mouse and their mean values were plotted using the plot_cpdb3 function from the ktplots R package (v.2.2.0) (<https://github.com/zktuong/ktplots>).

Bulk RNA-Seq data processing. From raw fastq files the reads with adapter contamination were excluded. After that the reads were aligned with HISAT2 v2.2.1 to the GRCm39 genome annotation¹⁶. The gene counts were calculated with htseq-count package v0.11.1¹⁷. For the

differential gene expression analysis the package DESeq2 v1.42.0 was used¹⁸. For the further DE analysis only protein-coding genes were taken. The volcano plots were prepared with the EnhancedVolcano package v1.20.0 (<https://github.com/kevinblighe/EnhancedVolcano>).

Pathway enrichment analysis. For gene-set enrichment analysis (GSEA), genes were pre-ranked in decreasing order by the absolute values of logFC. GSEA was performed on this pre-ranked list using the R package clusterProfiler v4.10.1 with default parameters and the GO Biological Process database ('BP')¹⁹. Custom gene sets for GSEA were generated using results from bulk RNA-Seq analyses of HCA-7 cell lines after rhOSM stimulation (24h stimulation). The selection process focused on identifying statistically significant upregulated DEGs with $\text{padj} < 0.05$. Similarly, for the HCA-7 cell line dataset, DEGs with a logFC greater than 0.5 were selected (**Supplementary table 6**). The results were filtered for significantly enriched gene sets (Benjamini-Hochberg-adjusted $P < 0.05$).

Plotting and statistical analysis. Statistical analysis and visualization were performed using R version 4.1.2 and 4.3.1. Statistical significance tests were performed as described in each figure legend. Unless stated otherwise, all tests were significant with FDR-adjusted $P < 0.05$. Plots were generated with the R package ggplot2.

Xenium in Situ analysis. Xenium *in situ* analysis (10X Genomics) was conducted utilising a custom gene panel that included *OSM*, *OSMR* and several canonical epithelial (*EPCAM*, *CDH1*, *KRT20*, *MUC5B*, *MKI67*) and non-epithelial genes (*CD3E*, *CD4*, *CD14*, *CD68*, *CIQC*, *CD19*, *CD79A*, *PDGFRA*, *VIM*, *PECAMI*, *CD34*, *KIT*). Samples were prepared according to the manufacturer's guidelines (CG000578, Rev D). Human colitis-associated cancer (CAC) and healthy colon (HC) FFPE blocks (**Supplementary table 8**) were sectioned at a thickness of 5 μm , followed by mounting it on Xenium slides. These sections were processed according to manufacturer's guidelines (CG000760, Rev A). Briefly, the sections underwent sequential deparaffinization and permeabilization, followed by overnight hybridisation with custom probes

at 50°C. After post-hybridization washes, we performed probe amplification and multimodal staining for cell membrane and nucleus detection. Next, autofluorescence quenching was done and the slides were loaded into the Xenium Analyzer. After the run completion, H&E stainings were performed as per Xenium guidelines (CG000613, B). H&E images were acquired using a BZ-X810 microscope (Keyence) using a 20x air objective.

Xenium Data processing and analysis. Raw Xenium transcript data were initially processed using Xenium Ranger v3.1.1 according to the manufacturer's guidelines. Subsequent analysis and visualization were performed using the Python package Squidpy (v1.2.2)²⁰ and Scanpy (v1.10.1)²¹. After basic quality control and filtering out low quality cells from individual patients, cells were classified into epithelial and non-epithelial lineages. To compare the spatial expression of OSM and OSMR between CAC and UC, counts were normalized by tissue surface area (counts per μm^2). Within the epithelial cell population, we examined and plotted OSMR expression, while OSM expression was examined in non-epithelial cells. For spatial visualization of gene expression, H&E images were imported and aligned to the DAPI-stained images using Xenium Explorer (v3.2.0), through manual placement of 10-12 keypoints on each image. Following alignment, transcripts were overlaid onto the H&E image. Final images were exported using the platform's export image function.

SUPPLEMENTARY REFERENCES

1. Picelli, S. *et al.* Full-length RNA-seq from single cells using Smart-seq2. *Nat. Protoc.* **9**, 171–181 (2014).
2. Picelli, S. *et al.* Smart-seq2 for sensitive full-length transcriptome profiling in single cells. *Nat. Methods* **10**, 1096–1098 (2013).
3. Hao, Y. *et al.* Dictionary learning for integrative, multimodal and scalable single-cell analysis. *Nat. Biotechnol.* **42**, 293–304 (2024).
4. Korsunsky, I. *et al.* Fast, sensitive and accurate integration of single-cell data with Harmony. *Nat. methods* **16**, 1289–1296 (2019).
5. Kinchen, J. *et al.* Structural Remodeling of the Human Colonic Mesenchyme in Inflammatory Bowel Disease. *Cell* **0**, 372–386.e17 (2018).
6. Smillie, C. S. *et al.* Intra- and Inter-cellular Rewiring of the Human Colon during Ulcerative Colitis. *Cell* **178**, 714–730.e22 (2019).
7. Kong, L. *et al.* The landscape of immune dysregulation in Crohn’s disease revealed through single-cell transcriptomic profiling in the ileum and colon. *Immunity* **56**, 444–458.e5 (2023).
8. Ewels, P. A. *et al.* The nf-core framework for community-curated bioinformatics pipelines. *Nat. Biotechnol.* **38**, 276–278 (2020).
9. Dobin, A. *et al.* STAR: ultrafast universal RNA-seq aligner. *Bioinformatics* **29**, 15–21 (2013).
10. Patro, R., Duggal, G., Love, M. I., Irizarry, R. A. & Kingsford, C. Salmon provides fast and bias-aware quantification of transcript expression. *Nat. Methods* **14**, 417–419 (2017).
11. Pavlidis, P. *et al.* Interleukin-22 regulates neutrophil recruitment in ulcerative colitis and is associated with resistance to ustekinumab therapy. *Nat. Commun.* **13**, 5820 (2022).
12. Barbie, D. A. *et al.* Systematic RNA interference reveals that oncogenic KRAS-driven cancers require TBK1. *Nature* **462**, 108–12 (2009).
13. Holland, C. H. *et al.* Robustness and applicability of transcription factor and pathway analysis tools on single-cell RNA-seq data. *Genome Biol.* **21**, 36 (2020).
14. Gu, Z., Eils, R. & Schlesner, M. Complex heatmaps reveal patterns and correlations in multidimensional genomic data. *Bioinformatics* **32**, 2847–2849 (2016).
15. Efremova, M., Vento-Tormo, M., Teichmann, S. A. & Vento-Tormo, R. CellPhoneDB: inferring cell–cell communication from combined expression of multi-subunit ligand–receptor complexes. *Nat Protoc* **15**, 1484–1506 (2020).
16. Kim, D., Paggi, J. M., Park, C., Bennett, C. & Salzberg, S. L. Graph-based genome alignment and genotyping with HISAT2 and HISAT-genotype. *Nat. Biotechnol.* **37**, 907–915 (2019).
17. Anders, S., Pyl, P. T. & Huber, W. *HTSeq - A Python Framework to Work with High-Throughput Sequencing Data*. <http://biorxiv.org/lookup/doi/10.1101/002824> (2014).
18. Love, M. I., Huber, W. & Anders, S. Moderated estimation of fold change and dispersion for RNA-seq data with DESeq2. *Genome Biol.* **15**, 550 (2014).
19. Wu, T. *et al.* clusterProfiler 4.0: A universal enrichment tool for interpreting omics data. *Innov.* **2**, 100141 (2021).
20. Palla, G. *et al.* Squidpy: a scalable framework for spatial omics analysis. *Nat. Methods* **19**, 171–178 (2022).

21. Wolf, F. A., Angerer, P. & Theis, F. J. SCANPY: large-scale single-cell gene expression data analysis. *Genome Biol.* **19**, 15 (2018).

SUPPLEMENTARY FIGURES

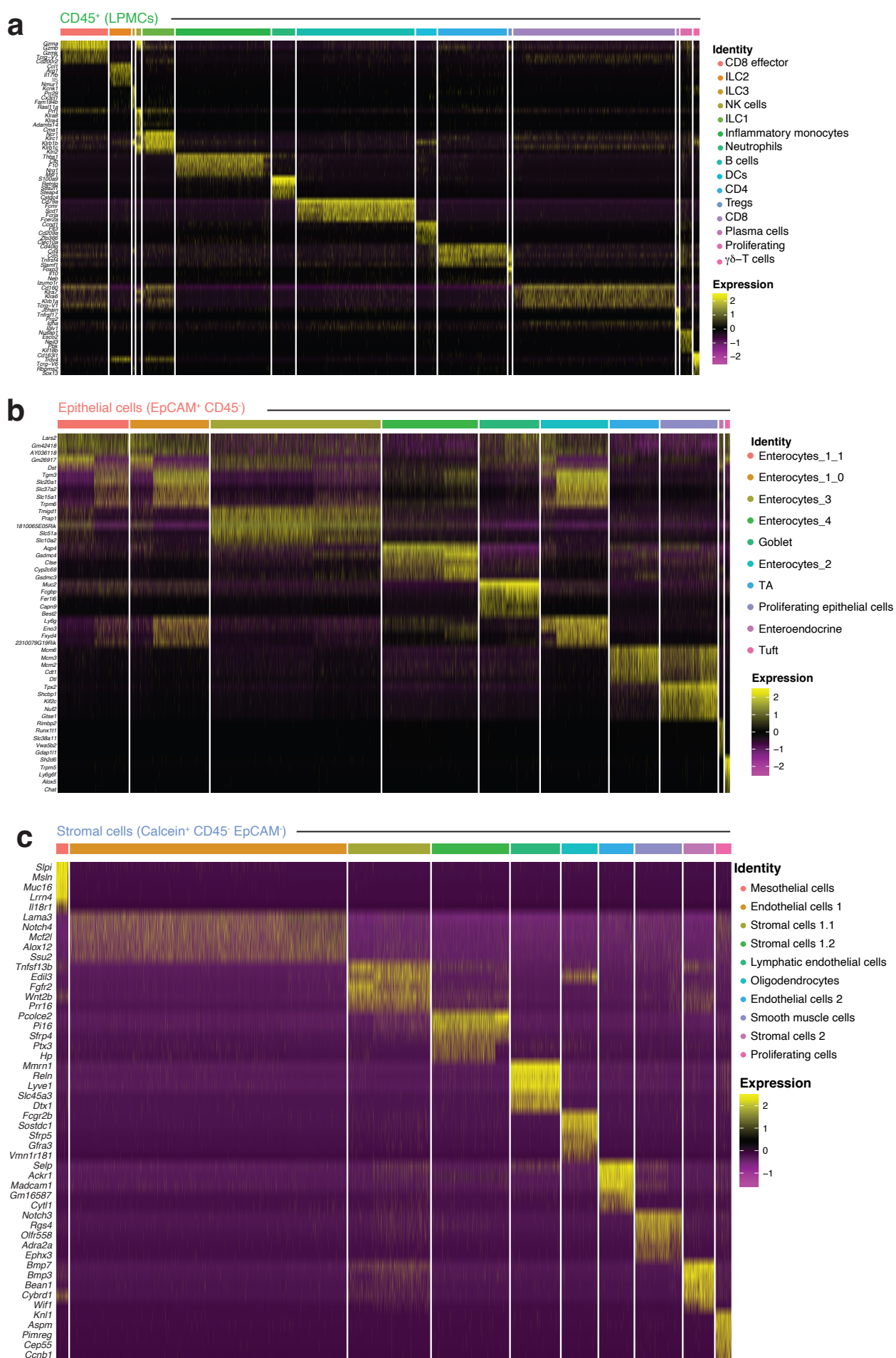


Figure S1. Cell subset-specific features of the mouse colon single-cell analysis.

- (a) Heatmap showing scaled gene expression of the top five genes representing each of the fourteen cell types found in the CD45⁺ LPMC. Each column displays gene expression from an individual cell, and genes are listed in the rows.
- (b) Heatmap of differentially expressed genes in epithelial cell clusters.
- (c) Heatmap of differentially expressed genes in stromal cell clusters.

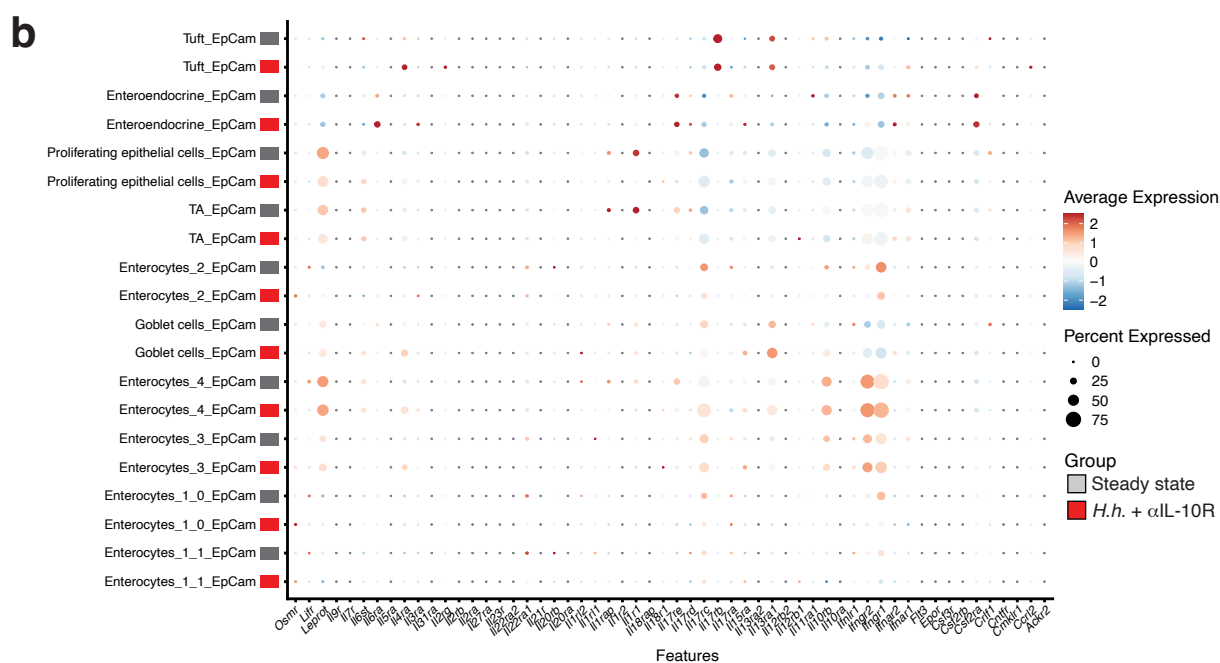
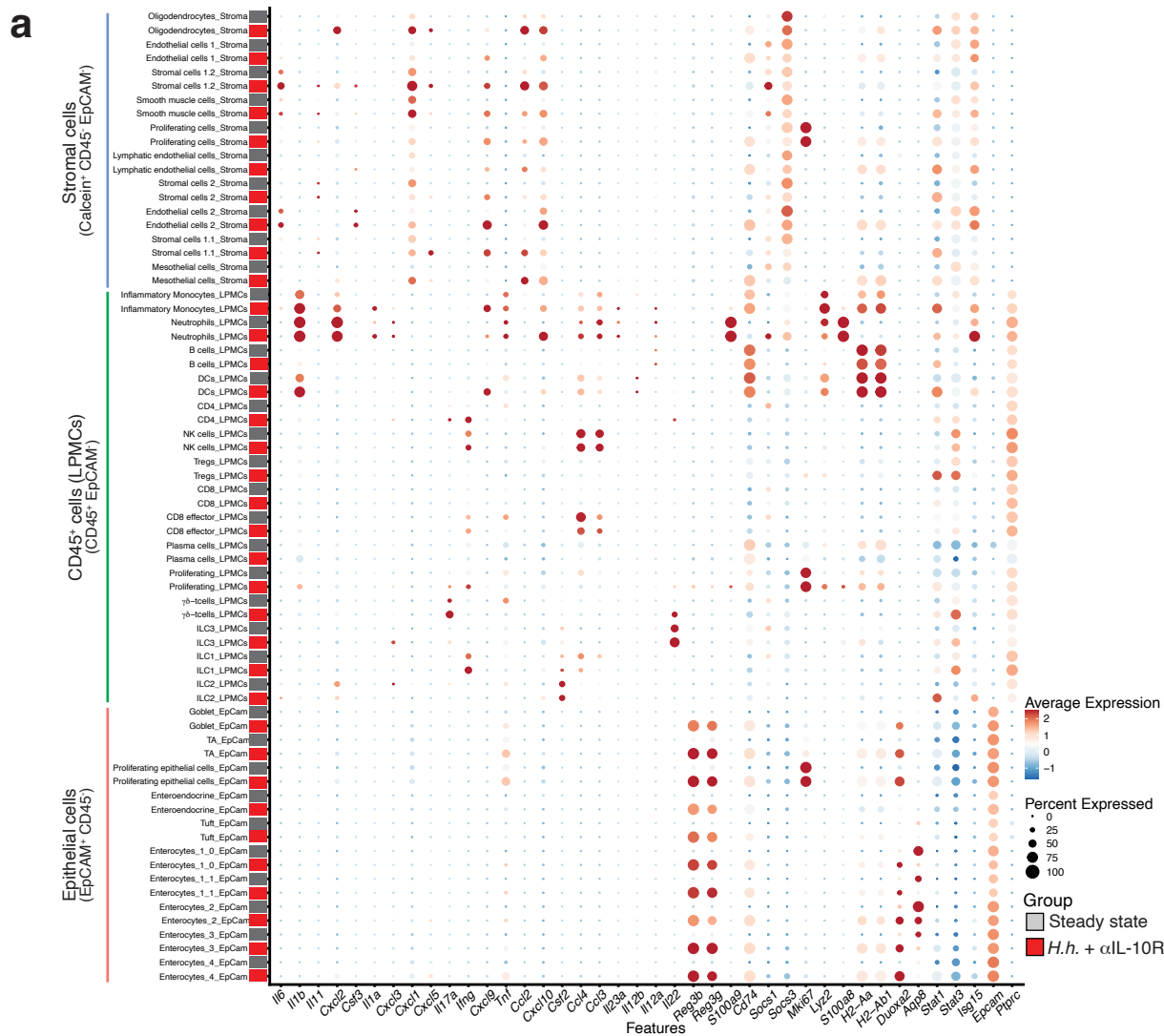


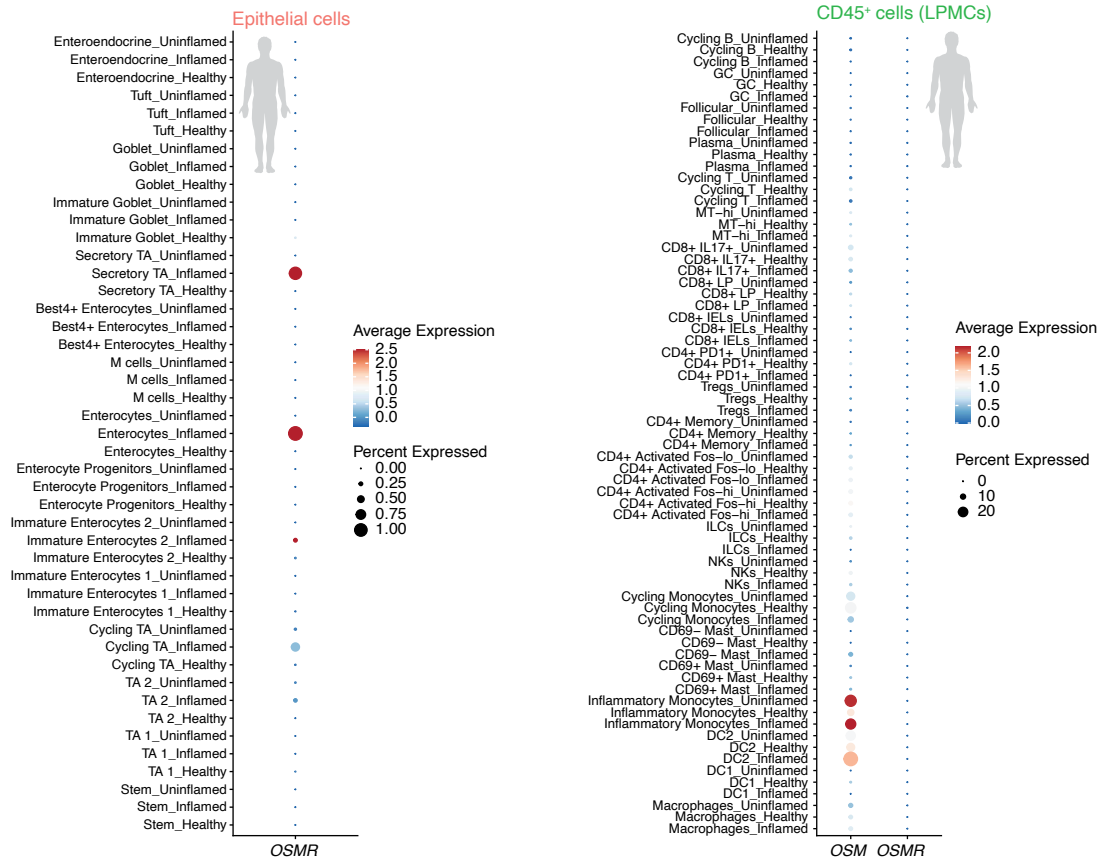
Figure S2

Figure S2. Expression of inflammatory genes and cytokine receptors in colon-resident cells.

(a) scRNA-seq dot plot depicting the expression profiles of various cytokines, chemokines, and other genes related to the pathogenesis of IBD. Red labels in the rows represent cell clusters from the inflamed condition; gray labels, steady-state condition.

(b) scRNA-seq dot plot depicting the expression profiles of cytokine receptors in epithelial cells. Red labels in the rows represent cell clusters from the inflamed condition; gray labels, steady-state condition.

a



b

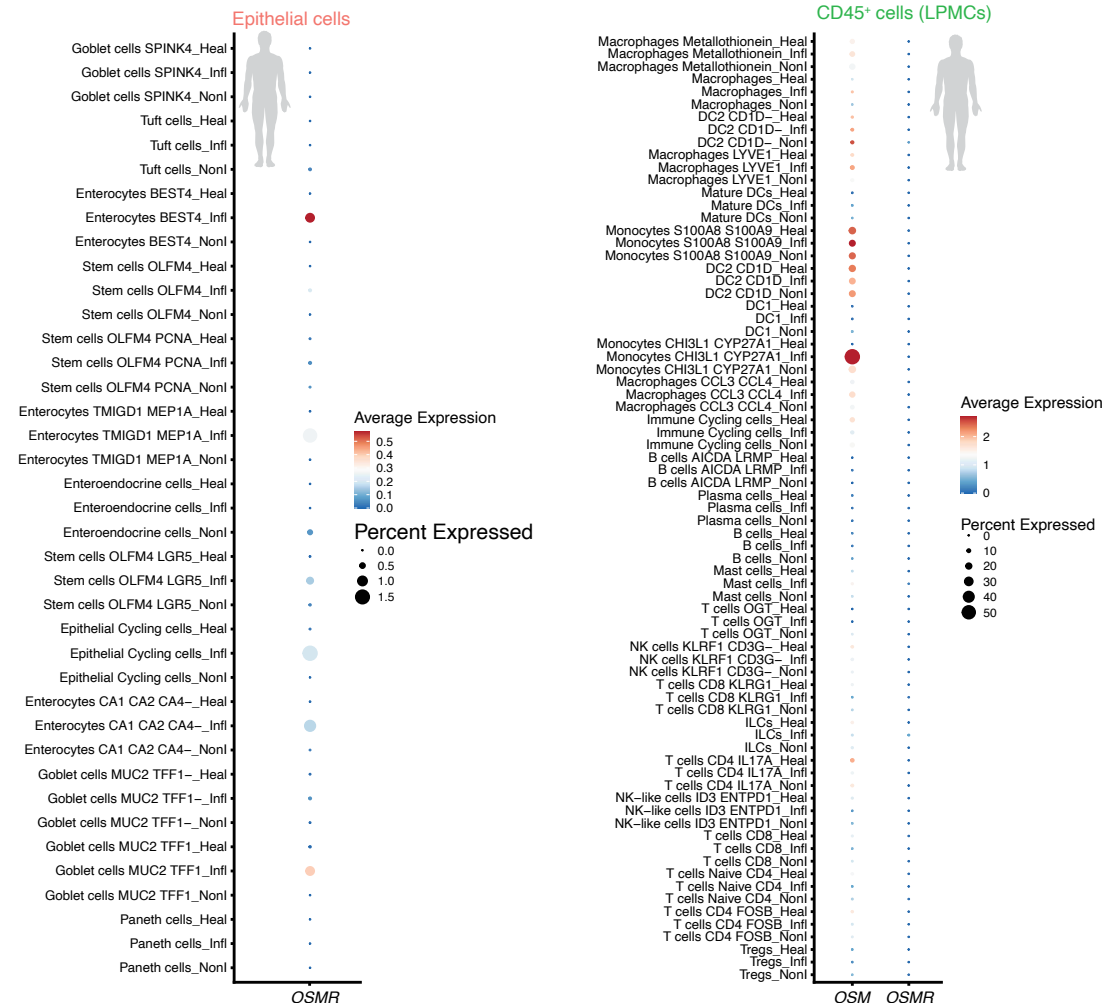


Figure S3

Figure S3. Expression of *OSM* and *OSMR* in healthy controls, ulcerative colitis, and Crohn's disease.

(a) scRNA-seq dot plot representing the expression profiles of *OSM* and *OSMR* in human epithelial and CD45⁺ cells in UC. Gene expression of *OSM* and *OSMR* is shown for cell clusters from patients with UC (inflamed and uninfamed samples) and healthy control patients. Data derived from Smillie et al.⁶.

(b) scRNA-seq dot plot representing the expression profiles of *OSM* and *OSMR* in human epithelial and CD45⁺ cells in Crohn's disease. Gene expression of *OSM* and *OSMR* is shown for cell clusters from patients with Crohn's disease (inflamed and uninfamed samples) and healthy control patients. Data derived from Kong et al.⁷.

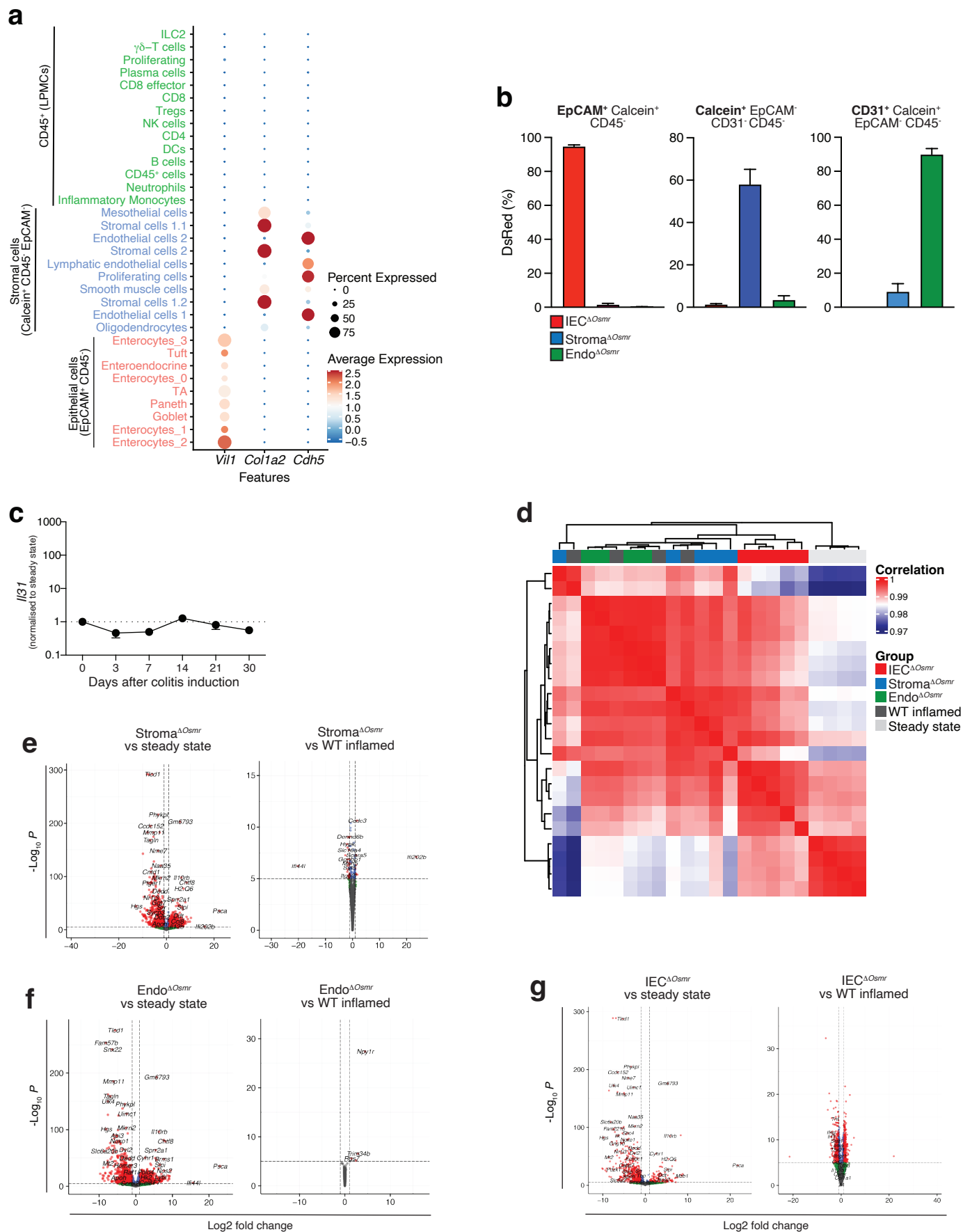


Figure S4. Gene expression profiling of colonic tissue in cell type-specific deletion of OSMR.

(a) scRNA-seq dot plot depicting the expression of *Vill*, *Colla2*, and *Cdh5* in the different cell types.

(b) *Vil^{creERT2} Ai9*, *Colla2^{creERT2} Ai9*, and *Cdh5^{cre} Ai9* mice were treated with tamoxifen, and the expression of DsRed was evaluated in the expected cell populations to assess the deletion efficiency of the different deleter lines. Data derive from one experiment (n=3-5).

(c) *Il31* expression in the colonic tissue in inflamed mice normalized to steady-state mice (day 3, n=7; day 14, n=8; day 21, n=8; day 31, n=8). Data represent mean \pm SEM, from 2 independent experiments.

(d) Clustered correlation heatmap of inflamed IEC $\Delta Osmr$, Stroma $\Delta Osmr$, and Endo $\Delta Osmr$ knockouts and control mice as well as steady-state mice based on their gene expression profiles.

(e) Volcano plot depicting differentially expressed genes in whole colon tissue between inflamed Stroma $\Delta Osmr$ cells and inflamed WT mice or steady-state control mice (n=4-5 per group). Red dots represent genes expressed more than 2 fold with statistical significance $p < 0.05$.

(f) Volcano plot depicting differentially expressed genes in whole colon tissue between inflamed Endo $\Delta Osmr$ cells and inflamed WT mice or steady-state control mice (n=4-5 per group). Red dots represent genes expressed at high levels with statistical significance.

(g) Volcano plot depicting differentially expressed genes in whole colon tissue between inflamed IEC $\Delta Osmr$ cells and inflamed WT mice or steady-state control mice (n=4-5 per group). Red dots represent genes expressed at high levels with statistical significance.

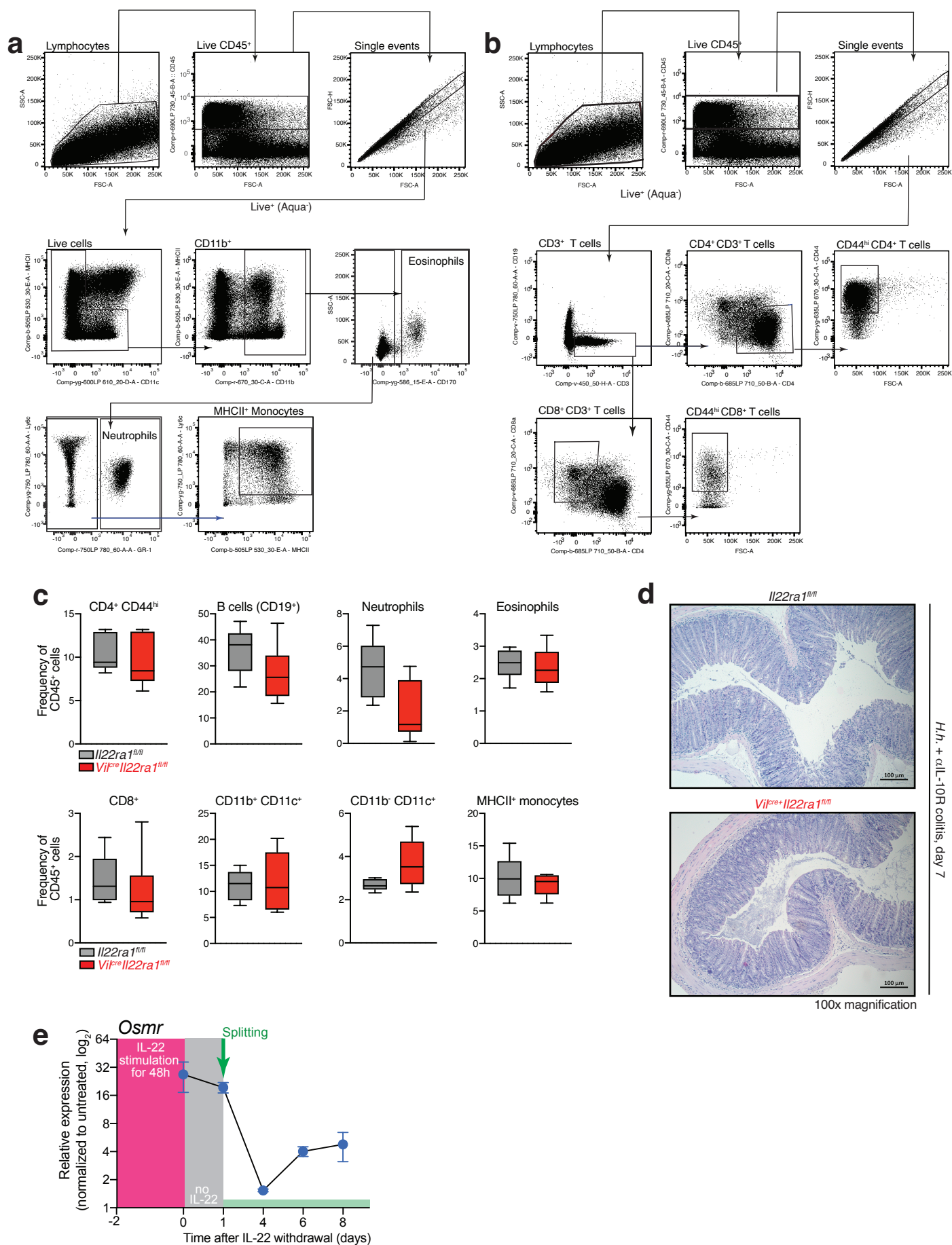


Figure S5

Figure S5. Flow cytometry analysis of immune cell compartment in *Vil^{Cre} Il22ra^{fl/fl}* mice during colitis.

(a, b) Gating strategies to identify the different myeloid (a) and lymphocytic (b) immune cell populations.

(c) Frequency of immune cell subtypes among total live CD45⁺ cells from colon lamina propria of inflamed *Vil^{Cre-}Il22ra^{fl/fl}* and *Vil^{Cre+}Il22ra^{fl/fl}* mice. Live CD45⁺ colonic cells were identified. Eosinophils were distinguished by Siglec-F expression. Neutrophils were characterized as Ly6C⁺/GR1⁺ and MHCII⁺ monocytes as Ly6C⁺/MHCII⁺. Additionally, CD44^{high}/CD4⁺ and CD44^{high}/CD8⁺ T cell populations were evaluated. Data are representative of a single independent experiment; n=6 mice per genotype.

(d) Representative H&E-stained colon sections from *Vil^{Cre+}Il22ra^{fl/fl}* and *Vil^{Cre-}Il22ra^{fl/fl}* mice on day 7 post-colitis induction; n=6 mice per genotype. Scale bar 100 μ m.

(e) *Osmr* expression stability was tested by stimulating colon epithelial organoids with 10 ng/mL of IL-22 for 48 h. The organoids were then washed, passaged, and cultured in medium without IL-22. Samples were collected at the indicated time points for q-PCR analysis. Data is representative of two independent experiments.

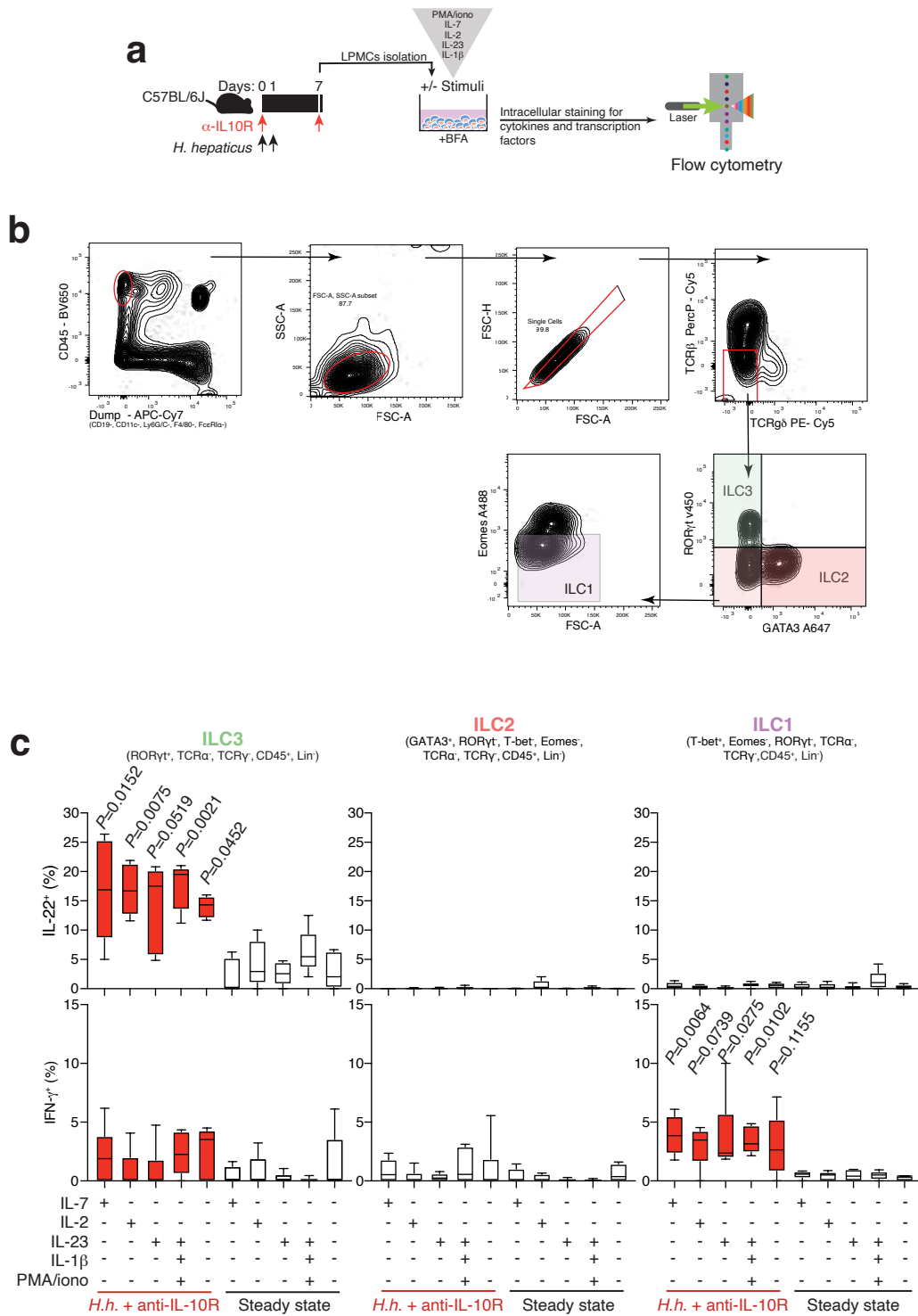


Figure S6

Figure S6. Optimisation of innate lymphoid cell activation and cytokine production.

(a) Experimental design for the *H.h.*+ anti-IL-10R colitis model and analysis of lamina propria innate lymphoid cells (ILCs). C57BL/6J mice were treated with anti-IL-10R and infected with *H.h.* for seven days before analysis. Lamina propria mononuclear cells (LPMCs) were isolated from inflamed ($n=6$) and steady-state ($n=6$) mice, stimulated *ex vivo* under the indicated conditions, and analyzed for cytokine and transcription factor expression by flow cytometry.

(b) Gating strategy for identifying ILC subsets in colonic LPMCs. Sequential gating was performed to exclude doublets, dead cells, and lineage-positive cells. ILCs were identified based on CD90.2 (Thy1) expression and further classified into ILC3 (ROR γ t⁺), ILC2 (GATA3⁺), and ILC1 (T-bet⁺) subsets.

(c) Bar graphs (mean \pm SEM) show the percentage of cytokine-producing cells among ILC3 (left), ILC2 (middle), and ILC1 (right) subsets upon stimulation with the indicated conditions. Statistical analysis was performed using the Kruskal-Wallis test, with comparisons made to the steady-state group.

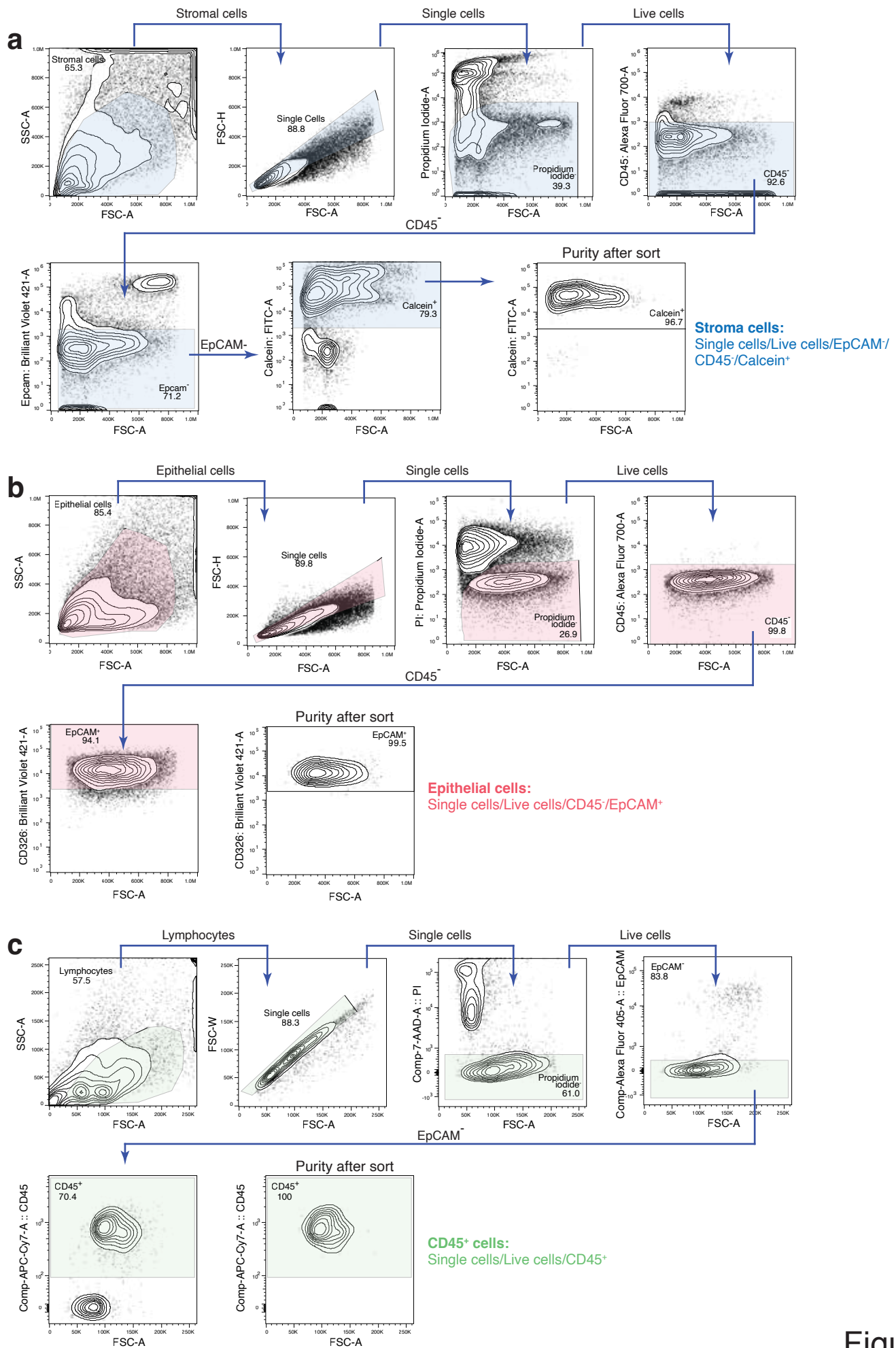


Figure S7

Figure S7. Fluorescence-activated cell sorting of CD45⁺, epithelial and stromal cells from colon tissue.

- (a) Sorting strategy of stromal cells and purity control after sorting are shown.
- (b) Sorting strategy of epithelial cells and purity control after sorting are shown.
- (c) Sorting strategy of immune CD45⁺ cells and purity control after sorting are shown.